

**Marquette University**  
**e-Publications@Marquette**

---

Civil and Environmental Engineering Faculty  
Research and Publications

Civil and Environmental Engineering, Department  
of

---

5-1-2012

# Resonant Characteristics of Rectangular Microcantilevers Vibrating Torsionally in Viscous Liquid Media

Tao Cai  
*Marquette University*

Fabien Josse  
*Marquette University, fabien.josse@marquette.edu*

Isabelle Dufour  
*Université de Bordeaux*

Stephen M. Heinrich  
*Marquette University, stephen.heinrich@marquette.edu*

Nicholas J. Nigro  
*Marquette University, nicholas.nigro@marquette.edu*

*See next page for additional authors*

---

Accepted Version Published as part of the proceedings of the conference, *2012 IEEE International Frequency Control Symposium*, 2012: 1-6. DOI. © 2012 Institute of Electrical and Electronics Engineers (IEEE). Used with permission

---

**Authors**

Tao Cai, Fabien Josse, Isabelle Dufour, Stephen M. Heinrich, Nicholas J. Nigro, and Oliver Brand

# Resonant characteristics of rectangular microcantilevers vibrating torsionally in viscous liquid media

Tao Cai

*Department of Electrical and Computer Engineering, Marquette University  
Milwaukee, Wisconsin*

Fabien Josse

*Department of Electrical and Computer Engineering, Marquette University  
Milwaukee, Wisconsin*

Stephen Heinrich

*Department of Civil Construction and Environmental Engineering, Marquette University  
Milwaukee, Wisconsin*

Nicholas Nigro

*Department of Mechanical Engineering, Marquette University  
Milwaukee, Wisconsin*

Isabelle Dufour

*Université de Bordeaux, IMS, UMR5218  
Talence, France*

Oliver Brand

*School of Electrical and Computer Engineering, Georgia Institute of Technology  
Atlanta, Georgia*

**Abstract:** The resonant characteristics of rectangular microcantilevers vibrating in the torsional mode in viscous liquid media are investigated. The hydrodynamic load (torque per unit length) on the vibrating beam due to the liquid was first determined using a finite element model. An analytical expression of the hydrodynamic function in terms of the Reynolds number and aspect ratio,  $h/b$  (with thickness,  $h$ , and width,  $b$ ) was then obtained by fitting the numerical results. This allowed for the resonance frequency and quality factor to be investigated as functions of both beam geometry and medium properties. Moreover, the effects of the aspect ratio on the cross-section's torsional constant,  $K$ , which affects the microcantilever's torsional stiffness, and on its polar moment of inertia,  $J_p$ , which is associated with the beam's rotational inertia, are also considered when obtaining the resonance frequency and quality factor. Compared with microcantilevers under out-of-plane (transverse) flexural vibration, the results show that microcantilevers that vibrate in their 1st torsional or 1st in-plane (lateral) flexural resonant modes have higher resonance frequency and quality factor. The increase in resonance frequency and quality factor results in higher mass sensitivity and reduced frequency noise, respectively. The improvement in the sensitivity and quality factor are expected to yield much lower limits of detection in liquid-phase chemical sensing applications.

**IEEE Keywords:** Resonant frequency, Liquids, Hydrodynamics, Q factor, Geometry, Torque, Mathematical model

## **SECTION 1.**

### *Introduction*

Dynamically driven microcantilevers excited in the out-of-plane (or transverse) direction [1] are widely investigated and used as highly sensitive chemical sensor platforms in various applications. The shifts in the resonance frequency of the microcantilevers are used to measure the presence and concentration of a chemical analyte in the operating environment. While these devices operate well in air, they have limited applications in viscous liquid media. The combination of increased viscous damping and effective fluid mass due to the liquid medium significantly decreases the resonance frequency and quality factor of the device, thereby decreasing the mass sensitivity of the system and increasing the susceptibility of the system to frequency noise. In order to improve these characteristics, it has been proposed

to investigate other vibration modes of microcantilevers, such as the in-plane (lateral) flexural mode [2][3][4] or torsional mode [5].

While microcantilevers vibrating in the out-of-plane flexural mode in viscous liquids are being extensively investigated, there is limited work on the torsionally vibrating cantilevers in the literature. Microcantilevers torsionally vibrating in vacuum have been investigated; their resonance frequency has been obtained in a closed-form analytical expression from the equation of motion of the vibrating microcantilever, in terms of the geometry and material properties of the microcantilever [5][6][7]. A closed-form analytical expression for the torsional resonance frequency [8] has also been obtained in inviscid liquids, with the pressure effect of the liquid accounted for in terms of the geometry and material properties of the micro-cantilever and the density of the liquid. This was done by solving the Navier-Stokes equations for inviscid liquids [8][9].

For a microcantilever torsionally vibrating in viscous liquids, both the pressure and viscous shear effects of the liquid must be taken into account. By calculating the fluid's resisting torque per unit length, an analytical expression for the hydrodynamic function of a circular cross-section micro cantilever in viscous liquids under torsional mode has been derived by Stokes [10] in terms of the Reynolds number. Green and Sader [5] proposed an analytical expression of the hydrodynamic function and set up the procedure to calculate the resonance frequency and quality factor of a rectangular microcantilever with negligible thickness (ribbon case) in viscous liquids under the torsional mode. In the approach, the hydrodynamic function only depends on the Reynolds number and does not account for the thickness. The solution was obtained by solving the Navier-Stokes equations for viscous liquids [5][9], using the numerical integral method introduced by Tuck [11].

In the present study, the characteristics of torsionally vibrating rectangular microcantilevers in viscous liquids are investigated taking into account the thickness effects on the hydrodynamic function, the polar moment of area, and the torsional constant. The values of the hydrodynamic function are obtained by using numerical simulations for different Reynolds numbers and aspect ratios. An analytical expression

for the hydrodynamic function in terms of both the Reynolds number and aspect ratio are obtained by surface fitting the numerical results. The effects of the hydrodynamic torque on the resonance frequency and quality factor are then investigated with respect to the microcantilever geometry and the material properties of the cantilever and the liquid. Trends in these characteristics as a function of the geometric parameters and/or material properties are investigated for liquid-phase sensing applications.

## **SECTION II.**

### *Assumptions*

A typical rectangular microcantilever under torsional mode operation is shown in Fig. 1. In this study, the following assumptions are used:

1. The microcantilever deforms elastically, but for the purpose of calculating the hydrodynamic load it is assumed to be a rigidly rotating member.
2. The length of the microcantilever is much greater than its width  $b$  or thickness  $h$ : Thus, end effects are ignored.
3. The amplitude of the rotational deflections (rotation angles of cross sections) is assumed to be very small.
4. Mode coupling between different orders and types of vibrating modes is neglected.
5. The longitudinal inertia and longitudinal stress due to warping of the cross section will be neglected in developing the classical torsional model.
6. The liquid is incompressible and Newtonian.
7. The liquid domain is much larger than the size of the microcantilever.

8. The interface between the microcantilever and the liquid is a non-slip interface.
9. There is no source or sink of mass or heat in the fluid domain, and heat transfer effects are ignored.
10. Body forces (gravitational forces) are ignored.

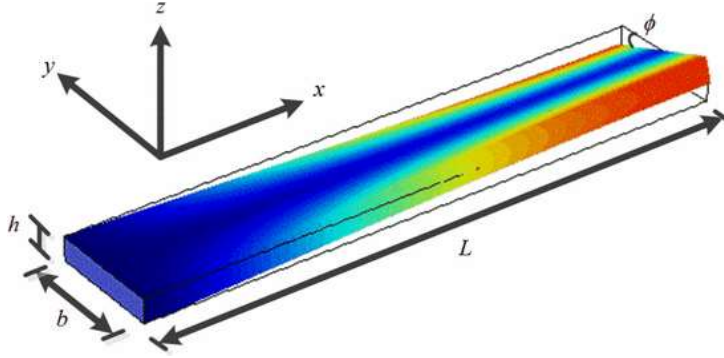


Figure 1  
Figure 1: Geometry of a microcantilever of length  $L$ , width  $b$ ; and thickness  $h$ , where  $\phi$  is the rotational deflection (angle). The color coding represents the  $z$ -axis deflection.

## SECTION III.

### *Theoretical analysis*

#### **A. Equation of Motion**

The equation of motion for the torsionally vibrating rectangular beam in a vacuum is given by

$$(1) \quad GK \frac{\partial^2 \phi(x,t)}{\partial x^2} - \rho J_p \frac{\partial^2 \phi(x,t)}{\partial t^2} = T_{drive}(x) e^{j\omega t},$$

where  $G$  is the shear modulus,  $K$  is the torsional constant.  $\rho$  is the mass density,  $J_p$  is the polar (area) moment of inertia of the beam cross section,  $\phi$  is the rotational deflection (angle),  $T_{drive}$  is the position-dependent excitation torque per unit length applied at an angular frequency of  $\omega$ .

When the beam is operating in a viscous liquid, an additional torque per unit length from the liquid affects the beam and the equation of motion is modified to

$$(2) \quad GK \frac{\partial^2 \phi(x, t)}{\partial x^2} - \rho J_p \frac{\partial^2 \phi(x, t)}{\partial t^2} = T_{\text{drive}}(x) e^{j\omega t} + T_{\text{hydro}}(x, \text{Re}, \frac{h}{b}),$$

with the Reynolds number expressed as

$$(3) \quad \text{Re} = \frac{\rho_\ell \omega b^2}{4\eta},$$

where  $\rho_l$  is the mass density and  $\eta$ . is the dynamic viscosity of the liquid; the torque per unit length is expressed as

$$(4) \quad T_{\text{hydro}}(x, \text{Re}, \frac{h}{b}) = g_{1,\text{tors}} \frac{\partial \phi(x, t)}{\partial t} + g_{2,\text{tors}} \frac{\partial^2 \phi(x, t)}{\partial t^2},$$

$$g_{1,\text{tors}} = \frac{\pi \rho_\ell b^4 \omega}{8} \Gamma_{\text{rect,tors,imag}}(\text{Re}, \frac{h}{b}),$$

$$g_{2,\text{tors}} = \frac{\pi \rho_\ell b^4}{8} \Gamma_{\text{rect,tors,real}}(\text{Re}, \frac{h}{b}),$$

where  $g_{1,\text{tors}}$  is the frequency-dependent coefficient associated with the liquid damping torque per unit length and is written in terms of the imaginary part of the hydrodynamic function, and  $g_{2,\text{tors}}$  is the frequency-dependent coefficient associated with the liquid inertial torque per unit length and is written in terms of the real part of the hydrodynamic function

$$(5) \quad \Gamma_{\text{rect,tors}}(\text{Re}, \frac{h}{b}) = \Gamma_{\text{rect,tors,real}}(\text{Re}, \frac{h}{b}) + j\Gamma_{\text{rect,tors,imag}}(\text{Re}, \frac{h}{b}),$$

which is a dimensionless complex-valued function depending on the Reynolds number and the aspect ratio, and obtained by solving the linearized Navier-Stokes equations for the liquid

$$(6) \quad \nabla \cdot \mathbf{v} = 0, \rho_\ell \frac{\partial \mathbf{v}}{\partial t} = -\nabla p + \eta \nabla^2 \mathbf{v},$$

where  $p$  and  $\mathbf{v}$  are the hydrodynamic pressure and velocity at a particular point in the liquid, respectively;  $\rho_l \partial \mathbf{v} / \partial t$ , is the term related to the liquid's inertial forces, while  $\eta \nabla^2 \mathbf{v}$ , is the term related to the liquid's viscous forces.



## B. Hydrodynamic Function

In order to calculate the resonance frequency of the system, an expression for the hydrodynamic function is required. An analytical expression for the hydrodynamic function of a micro cantilevers with circular cross-section in viscous liquids under torsional mode is well known and is given by (e.g. [5])

$$(7) \quad \Gamma_{\text{circ,tors}}(\omega) = \frac{2j}{\text{Re}} + \frac{jK_0(-j\sqrt{j\text{Re}})}{\sqrt{j\text{Re}K_1(-j\sqrt{j\text{Re}})}},$$

where  $K_0$  and  $K_1$  are modified Bessel functions of the third kind. Unfortunately, the relevant analytical expression for the hydrodynamic function of a micro cantilever with rectangular cross-section, which takes into account thickness effects, does not exist in the literature. An analytical expression based on curve-fitting numerical results for a rectangular microcantilever with negligible thickness, in terms of the Reynolds number, is obtained in [5]. In the present study, the thickness effect on the hydrodynamic function is investigated numerically using finite element models.

## C. Numerical Procedure

2D numerical simulations by COMSOL are used to extract the torque per unit length of the torsionally vibrating micro cantilevers in viscous liquids as a function of time. In these models, the rectangular cross-section of the microcantilever is assumed to be rigid with a constant width and variable thickness, and the surrounding liquid domain, a square with the same center as the cross-section of the micro cantilever, is modeled as incompressible fluid governed by the linearized Navier-Stokes equations in (6). On the inner boundary, an excited sinusoidal angular velocity is imposed. On the outer boundary, the pressure of the liquid and the viscous stress are set to zero. The amplitude of the exciting rotational velocity is held constant, while the excited frequency is varied in order to investigate the effects of different Reynolds numbers. The mass density and viscosity were set to those of water ( $\rho=1000 \text{ kg/m}^3$  and  $\eta=1 \text{ cP}$ ). A transient analysis is performed over three cycles, which is verified to be long enough to let the system reach steady state. The torque per unit length is then extracted as a function of time, and the magnitude, phase offset from

[2012 IEEE International Frequency Control Symposium (FCS), (May 2012): pg. 807-812. DOI. This article is © Institute of Electrical and Electronics Engineers (IEEE) and permission has been granted for this version to appear in [Publications@Marquette](mailto:Publications@Marquette). Institute of Electrical and Electronics Engineers (IEEE) does not grant permission for this article to be further copied/distributed or hosted elsewhere without the express permission from Institute of Electrical and Electronics Engineers (IEEE).]

the imposed angular velocity; the real and imaginary parts of the hydrodynamic function are then calculated.

A convergence study was performed to identify an appropriate mesh size and distribution. The mesh size is much smaller around the microcantilever's cross-section since higher gradients occur near the microcantilever. The thickness of the microcantilever and the excitation frequency were varied in different models to find the real and imaginary parts of hydrodynamic function in terms of both the Reynolds number,  $Re$ , and aspect ratio  $h/b$ .

#### D. Resonance Frequency

By solving the equation of motion (2), the frequency response of the system can be obtained. If the torsionally vibrating microcantilever is in vacuum, the  $i$ -th natural frequency is [6]

$$(8) \quad \omega_{\text{vac},i} = \lambda_i \sqrt{\frac{GK}{\rho J_p}}, \lambda_i = \frac{(2i-1)}{2L} \pi.$$

If the microcantilever is immersed in an inviscid liquid, the  $i$ -th resonance frequency is [8]

$$(9) \quad \omega_{\text{InvL},i} = 2\pi f_{\text{InvL},i} = \omega_{\text{vac},i} \left(1 + \frac{3\pi\rho_\ell b}{32\rho h}\right)^{-1/2}.$$

If the microcantilever is immersed in a viscous liquid, assuming that only the  $i$ -th torsional mode is excited and that the vibration shape is given by the  $i$ -th undamped mode shape  $\sin(\lambda_i x)$ , that is,

$$(10) \quad T_{\text{drive}}(x) = T_{\text{drive},i} \sin \lambda_i x; \phi(x, t) = \Phi(t) \sin \lambda_i x,$$

the system behaves as a simple harmonic oscillator, so that Eq. (2) can be rewritten as

$$(11) \quad (\rho J_p + g_{2,\text{tors}}) \frac{\partial^2 \Phi(t)}{\partial t^2} + g_{1,\text{tors}} \frac{\partial \Phi(t)}{\partial t} + GK \lambda_i^2 \Phi(t) = T_{\text{drive},i} e^{j\omega t}.$$

The damping ratio and the resonance frequency associated with the  $i$ -th mode are obtained:

$$(12) \quad \xi_i = \frac{\Gamma_{\text{rect,tors,imag}}(\omega_{\text{VisL},i})}{\frac{16\rho J_p}{\pi\rho_\ell b^4} + 2\Gamma_{\text{rect,tors,real}}(\omega_{\text{VisL},i})},$$

$$\omega_{\text{VisL},i} = 2\pi f_{\text{VisL},i}$$

$$(13) \quad = \omega_{\text{vac},i} \left[ 1 + \frac{\pi\rho_\ell b^4}{8\rho J_p} \Gamma_{\text{rect,tors,real}}(\omega_{\text{VisL},i}) \right]^{-1/2} \sqrt{1 - 2\xi_i^2}.$$

When the energy loss is low,  $\xi_i \ll 1$ , the expression of the resonance frequency in (13) is reduced to that given in [5].

## E. Quality Factor

The quality factor is defined in terms of  $2\pi$  times the ratio of the peak energy stored in a vibrating system to the energy lost per cycle.

From (11), the quality factor can be obtained as

When the energy loss is low,  $\xi_i \ll 1$ , the expression of the quality factor in (14) is reduced to that given in [5] and is equal to  $1/(2\xi_i)$ .

$$(14) \quad Q_{\text{tors}} = \frac{1}{2\xi_i \sqrt{1 - 2\xi_i^2}}.$$

## F. Thickness Effects

When calculating the hydrodynamic function, the resonance frequency, and the quality factor for the ribbon case [5], the thickness effects were ignored. In the present study, the thickness effects on the hydrodynamic function,  $\Gamma$ ) the torsional constant,  $K$ :, and polar moment of area,  $J_p$ , are considered as follows:

$$(15) \quad \Gamma_{\text{rect,tors,imag}}(\omega_{\text{VisL},i}) = \Gamma_{\text{rect,tors,imag}}\left(\text{Re}, \frac{h}{b}\right),$$

$$(16) \quad K = \frac{2bh^3}{k_2}; J_p = \frac{b^3h + bh^3}{12}.$$

Values of the parameter  $k_2$  in terms of the aspect ratio  $h/b$  are given in Table I [12]. When ignoring the thickness effects, the hydrodynamic function is reduced to a function of the Reynolds number; the torsional constant is reduced to  $bh^3/3$ ; the polar moment of area is reduced to  $b^3h/12$  which are used in ribbon case [5].

TABLE I. Parameter  $k_2$  for torsional constant [12]

$h/b$	1	2/3	1/2	2/5	1/3	1/4	1/5	1/10	0
$k_2$	14.2	10.2	8.73	8.03	7.60	7.12	6.87	6.41	6

## SECTION IV.

### *Results and Discussions*

#### **A. Results of Numerical Simulation**

Numerical results for the real and imaginary parts of the hydrodynamic function in terms of the Reynolds number and aspect ratio  $h/b$  are shown in Figs. 2a & b, respectively. Results using the analytical hydrodynamic function for the ribbon case [5] are also shown on the same figure for comparison purpose. From the figure, it can be seen that, as the Reynolds number increases, both real and imaginary parts of the hydrodynamic function decrease rapidly. Also, as the aspect ratio  $h/b$  decreases, both the real and imaginary parts of the hydrodynamic function decrease and the numerical results approach the empirical analytical expression for the ribbon case [5].

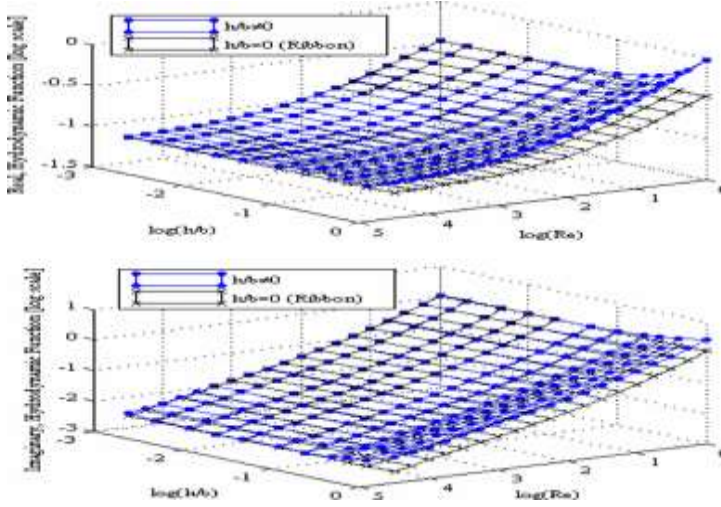


Figure 2: a) Real (above) and b) imaginary (below) parts of the hydrodynamic function in terms of the Reynolds number and aspect ratio.

## B. Analytical Approximation

An analytical form of the hydrodynamic function in terms of the Reynolds number,  $Re$ , and aspect ratio,  $h/b$ , is obtained by fitting the numerical results as follows,

$$(17) \quad \Gamma_{rect,tors,real} = (0.05 + 0.24Re^{-0.43})[1.2 + (h/b)^{0.89}],$$

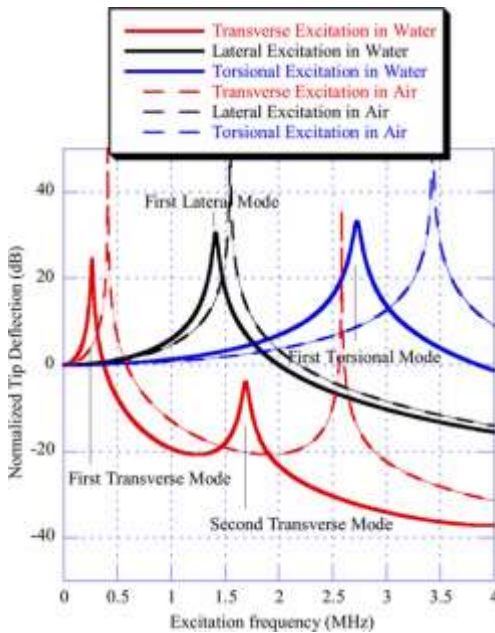
$$\Gamma_{rect,tors,imag} = (Re^{-1} + 0.45Re^{-0.5}) \left[ 0.75 + \left( \frac{h}{b} \right) \right],$$

With this analytical expression, one could rapidly obtain the hydrodynamic function for any arbitrary aspect ratio and Reynolds number within the parameter ranges investigated. For the investigated aspect ratios (from 0.01 to 0.2) and Reynolds numbers (from 1 to 31620), the real part of the hydrodynamic function is within 6.2% of the numerical results, and the imaginary part of the hydrodynamic function is within 22% of the numerical results. It is noted that the largest discrepancy for the imaginary part occurs when the Reynolds number is high and the aspect ratio is either very small or very large. When  $Re < 10000$  and  $0.02 \leq h/b \leq 0.1$ , the largest discrepancy between the imaginary parts of the expression and the numerical results decreases to 8%. A more complicated model could be used for fitting the imaginary part of the hydrodynamic function over a wide range of

Re and  $h/b$  For high Reynolds numbers, Although the relative errors are high, the absolute errors are small since the values of the imaginary part of the hydrodynamic function are very small.

### C. Frequency Spectrum

The solution to the equation of motion (2) can be used to calculate the magnitude of the tip rotation as a function of frequency for the microcantilever in air or water. For the calculations below, the Young's modulus, shear modulus and beam density are 169 GPa, 79.6 GPa, 2330 kg/m<sup>3</sup>, respectively; the density and viscosity of the air are 1.205 kg/m<sup>3</sup>, 0.01827 cP, respectively; the density and viscosity of the water are 1000 kg/m<sup>3</sup>, 1 cP, respectively. The simulated frequency spectra of a (200×45×12 μm) microcantilever vibrating torsionally, and transversely, laterally [3] in air and in water are shown in Fig. 3. For this specific geometry, the resonance frequency is higher for the first lateral and first torsional mode compared to the first transverse mode. The resonance frequencies of the first lateral and first torsional modes are higher due to the higher cantilever stiffness compared to the 1<sup>st</sup> transverse mode. The quality factors of the first lateral and first torsional mode are higher because the resonance frequency increases faster than the 3-dB bandwidth in these modes compared to the transverse mode.



[2012 IEEE International Frequency Control Symposium (FCS), (May 2012): pg. 807-812. DOI. This article is © Institute of Electrical and Electronics Engineers (IEEE) and permission has been granted for this version to appear in [Publications@Marquette](mailto:Publications@Marquette). Institute of Electrical and Electronics Engineers (IEEE) does not grant permission for this article to be further copied/distributed or hosted elsewhere without the express permission from Institute of Electrical and Electronics Engineers (IEEE).]

Figure 3: Simulated frequency spectra of a  $200 \times 45 \times 12 \mu\text{m}$  silicon microcantilever vibrating transversely, laterally, torsionally in air or water.

From Fig. 3, it is also seen that, for this microcantilever, the resonance frequency of the first torsional mode is not close to any other (transverse, lateral or torsional mode) resonance frequencies, indicating that no mode coupling is expected.

#### D. Resonance Frequency

The resonance frequency of a torsionally vibrating micro cantilever in vacuum calculated using (8) is found to be approximately proportional to  $h/(bL)$ . When operating in a viscous liquid media, the first resonance frequency of a torsionally vibrating microcantilever obtained using (12–13) is also found to have the same  $h/(bL)$  dependence. Fig. 4 compares the first resonance frequencies of torsionally vibrating microcantilevers as a function of  $h/(bL)$ , calculated using (12–13) and the method in [5]. The results indicate that the difference in the first torsional resonance frequencies is not negligible for  $h/b > 0.16$ , so that thickness effects cannot be neglected for these cantilever geometries.

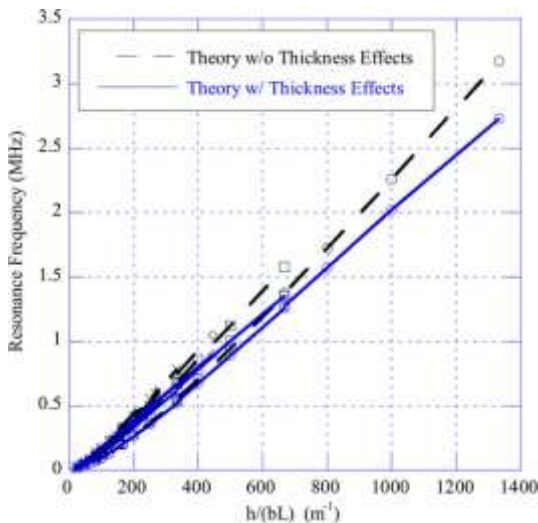


Figure 4: Simulated resonance frequency of silicon microcantilevers vibrating in the first torsional mode in water as a function of  $h/(bL)$  for widths of 45, 60, 75, and  $91 \mu\text{m}$ , lengths of  $200 \mu\text{m}$  (o),  $400 \mu\text{m}$  (□),  $600 \mu\text{m}$  (◇),  $800 \mu\text{m}$  (×),  $1000 \mu\text{m}$  (+) and thicknesses of 12, 6,  $3\frac{1}{2}$   $1.5 \mu\text{m}$ .



The values of the first resonance frequencies of several microcantilever geometries, considered in [2][3] vibrating transversely or laterally, are compared in Table II to those vibrating torsionally in air or in water. When operating in water, the first resonance frequency of a microcantilever vibrating transversely, laterally or torsionally is found to shift to a lower value, as expected. However, the predicted shifts are found to be different for all three vibration modes. For example, the first resonance frequencies of transversely and torsionally vibrating microcantilevers are predicted to decrease by as much as 50% and 32%, respectively, when placed in water. However, the first resonance frequency of the same beams vibrating laterally is predicted to only drop by a value of up to 10%. It is also shown in Table II that, for the same geometry, the first resonance frequency of laterally or torsionally vibrating microcantilevers in water is much higher than that of transversely vibrating microcantilevers. For liquid-phase chemical sensing applications, it is thus more advantageous to operate in the first in-plane (lateral) flexural mode or the first torsional mode because the sensitivity of a microcantilever as a chemical sensor is proportional to its resonance frequency.

TABLE II. First Resonance frequencies And Quality Factors Predicted For Three Sample Microcantilever Geometries

Geometry (Lxbxh) [ $\mu\text{m}$ ]	Transverse Mode [3]				Lateral Mode [3]				Torsional Mode			
	$f_{\text{air}}$ [MHz]	$f_{\text{water}}$ [MHz]	Percent Change	$Q_{\text{water}}$	$f_{\text{air}}$ [MHz]	$f_{\text{water}}$ [MHz]	Percent Change	$Q_{\text{water}}$	$f_{\text{air}}$ [MHz]	$f_{\text{water}}$ [MHz]	Percent Change	$Q_{\text{water}}$
400x45x12	0.103	0.064	-37.8%	9.30	0.386	0.347	-10.1%	17.1	1.717	1.355	-21.1%	31.5
200x45x12	0.412	0.264	-35.9%	17.3	1.547	1.411	-8.79%	34.3	3.433	2.726	-20.6%	44.5
200x90x12	0.412	0.214	-48.0%	22.7	3.095	2.934	-5.20%	60.0	1.847	1.276	-30.9%	44.3
200x45x6	0.206	0.102	-50.4%	9.1	1.547	1.443	-6.72%	21.2	1.847	1.257	-31.9%	22.24

## E. Quality Factor

The quality factor is evaluated using (12) and (14). The quality factors of microcantilever geometries considered in [2] [3] vibrating transversely, laterally and torsionally are compared in Table II. It is shown that, for the same geometry, the quality factor of microcantilevers vibrating in the first lateral or first torsional mode is much higher than that of micro cantilevers vibrating in the first transverse mode. It can be seen that the quality factors increase as



the length of the microcantilever decreases or as the thickness of the microcantilever increases for all three modes. However, as the width of the microcantilever decreases, the quality factors are also found to decrease for the transverse or lateral mode, whereas it remains almost constant for the torsional mode.

The quality factors of torsionally vibrating micro cantilevers calculated using (12) and (14) as a function of  $hL^{-0.5}$  are compared in Fig. 5 to those obtained in [5]. It is shown that the quality factors calculated by both methods are proportional to  $hL^{-0.5}$ . It is also seen that, as the aspect ratio  $h/b$  decreases, the calculated quality factors approach those calculated ignoring the thickness effects. However, for  $h/b > 0.16$ , the discrepancy between the two theories indicates that thickness effects become significant.

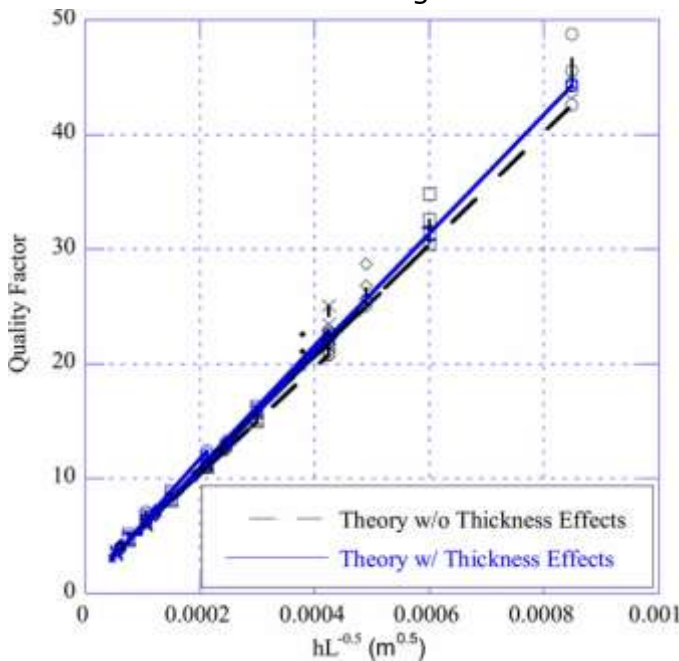


Figure 5: Simulated quality factor of silicon micro cantilevers vibrating in the first torsional mode in water as a function of  $hL^{-0.5}$  for widths of 45, 60, 75, and 90  $\mu\text{m}$ , lengths of 200  $\mu\text{m}$ ( $\circ$ ), 400  $\mu\text{m}$ ( $\square$ ), 600  $\mu\text{m}$ ( $\diamond$ ), 800  $\mu\text{m}$ ( $\times$ ), 1000  $\mu\text{m}$ ( $+$ ), and thicknesses of 12, 6, 3, 1.5  $\mu\text{m}$ .

## **SECTION V.**

### *Conclusions*

The resonance frequency and quality factor of torsionally vibrating microcantilevers in a viscous liquid medium were analyzed in terms of the beam's geometry and the properties of the liquid and compared to those of transversely or laterally vibrating microcantilevers.

The resonance frequency is found to be proportional to  $h/(bL)$  and the quality factor proportional to  $h/L\sqrt{\nu}$  for the torsionally vibrating microcantilever operating in a viscous liquid. The thickness effects on the hydrodynamic function, the polar moment of the area of the cross-section of the microcantilever, and the torsional constant affect the resonance frequency and the quality factor. For the selected geometries in water, thickness effects cannot be ignored when  $h/b > 0.16$ , especially for the resonance frequency (the errors of resonance frequency and quality factor could be greater than 10% and 5%, respectively). On the other hand, for the laterally vibrating microcantilevers, the resonance frequency is proportional to  $b/L^2$  and the quality factor is proportional to  $b\sqrt{\nu}/L$  [3]. Such different trends can be used to optimize device geometry and maximize frequency stability in chemical sensing applications.

Compared with microcantilevers under first transverse mode, micro cantilevers that vibrate in their first torsional or first lateral resonance modes have higher resonance frequency and quality factor. The increase in resonance frequency and quality factor results in higher sensitivity and reduced frequency noise, respectively. The improvement in the sensitivity and quality factor are expected to yield much lower limits of detection in liquid-phase chemical sensing applications.

### **References**

J. E. Sader, "Frequency response of cantilever beams immersed in viscous fluids with applications to the atomic force microscope". *Journal of Applied Physics*, 84(1), pp. 64-76, 1998.

[2012 IEEE International Frequency Control Symposium (FCS), (May 2012): pg. 807-812. [DOI](#). This article is © Institute of Electrical and Electronics Engineers (IEEE) and permission has been granted for this version to appear in [Publications@Marquette](mailto:Publications@Marquette). Institute of Electrical and Electronics Engineers (IEEE) does not grant permission for this article to be further copied/distributed or hosted elsewhere without the express permission from Institute of Electrical and Electronics Engineers (IEEE).]

- L. Beardslee, A.M. Addous, S.M. Heinrich, F. Josse, I. Dufour, and O. Brand, "Thermal Excitation and Piezoresistive Detection of Cantilever In-Plane Resonance Modes for Sensing Applications", *Journal of Microelectromechanical Systems*, 19(4), pp. 1015-1017, 2010.
- R. Cox, F. Josse, S. Heinrich, I. Dufour, O. Brand, "Resonant microcantilevers vibrating laterally in viscous liquid media", *IEEE International Frequency Control Symposium (IFCS)*, pp. 85-90, June 2010.
- R. Cox, F. Josse, S. M. Heinrich, O. Brand, I. Dufour, "Characteristics of laterally vibrating resonant microcantilevers in viscous liquid media", *Journal of Applied Physics*, 111, 014907, 2012.
- C. P. Green and J. E. Sader, "Torsional frequency response of cantilever beams immersed in viscous fluids with applications to the atomic force microscope", *Journal of Applied Physics*, 92, 10, 6262, 2002.
- L. D. Landau and E. M. Lifshitz, *Theory of Elasticity*, Pergamon, London, 1959.
- R. J. Roark, *Formulas for Stress and Strain*, McGraw-Hill, New York, 1943.
- W.-H. Chu, Technical Report No. 2, DTMB, Contract Nobs-86396(X), Southwest Research Institute, San Antonio, Texas, 1963.
- G. K. Batchelor, *Introduction to Fluid Dynamics*, New York: Cambridge University Press, 1977.
- G. G. Stokes, "On the Effect of the Rotations of the Cylinders or Spheres round their own Axes in increasing the Logarithmic Decrement of the Arc of Vibration", *Math. Phys. Pap.* 5, 207, 1886.

**NOT THE PUBLISHED VERSION; this is the author's final, peer-reviewed manuscript.** The published version may be accessed by following the link in the citation at the bottom of the page.

E.O Tuck, "Calculation of Unsteady Flows Due to small motions of cylinders in a viscous fluid", *Journal of Engineering Mathematics*, 3, 1, January 1969.

Sokolnikoff, *Mathematical Theory of Elasticity*, 2nd ed., pp. 128.

[2012 IEEE International Frequency Control Symposium (FCS), (May 2012): pg. 807-812. [DOI](#). This article is © Institute of Electrical and Electronics Engineers (IEEE) and permission has been granted for this version to appear in [e-Publications@Marquette](#). Institute of Electrical and Electronics Engineers (IEEE) does not grant permission for this article to be further copied/distributed or hosted elsewhere without the express permission from Institute of Electrical and Electronics Engineers (IEEE).]